BDS Wakefieleds simulation, issues and challenges for ILC and CLIC

P. Korysko
University of Oxford
CERN

Outline

- Intensity-dependent effects in ATF2

  - Simulation conditions.
  - Comparison between measurements and simulations.

- Intensity-dependent effects in the ILC.

  - Impact of short-range wakefields on the vertical beam size at the IP in both 250 GeV and 500 GeV ILC BDS.
  - Impact of long-range wakefields on the vertical beam deflection at the IP and the luminosity in both 250 GeV and 500 GeV ILC BDS.

- Intensity-dependent effects in CLIC.

  - Impact of short-range wakefields on the vertical beam size at the IP in the 380 GeV CLIC BDS.
  - Impact of long-range wakefields on the vertical beam deflection at the IP and the luminosity in the 380 GeV CLIC BDS.

- Conclusions

The Accelerator Test Facility (ATF2)

ATF2 layout, Twiss and parameters

ATF2 is a test facility to study the feasibility of the Final Focus System [1] that is envisaged in the future linear colliders CLIC and ILC. The primary project goal is to establish the hardware and beam handling technologies pertaining to transverse focussing of the electron beams to 37 nm. All the parameters can be found in the ATF2 design proposal report [2].

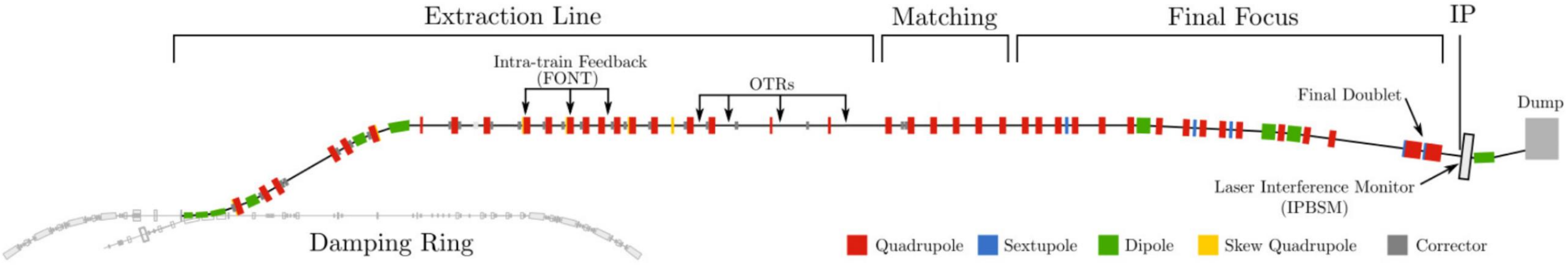

Table : Beam and optics parameters for ATF2 beamline.

Parameter	Symbol	Value
Length of ATF2	L	90 m
Beam energy	E	1.28 GeV
Bunch population	N_e	1.0×10^{10}
Beta functions at IP	β_x^*/β_y^*	40 mm/0.10 mm
Beam sizes at IP	σ_x^*/σ_y^*	8.9 µm/37 nm
Bunch length	σ_z	7 mm

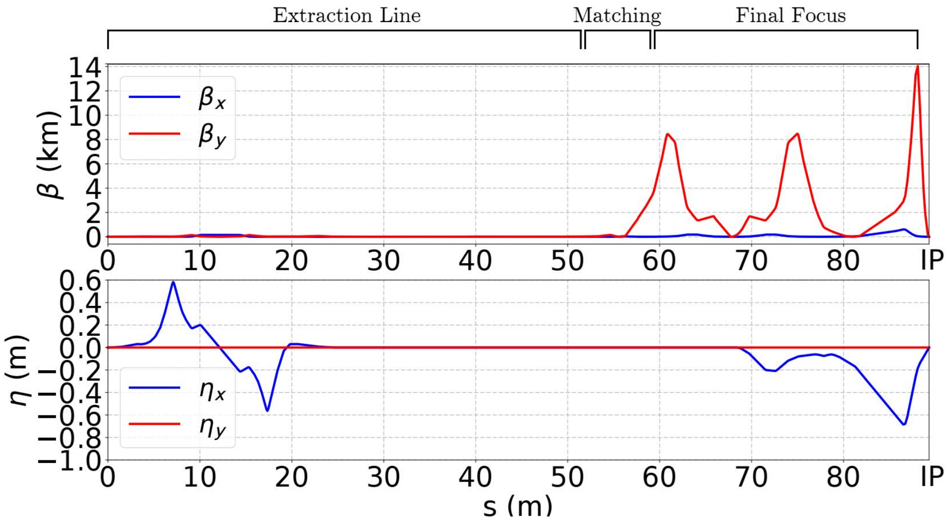

Introduction
Transverse and longitudinal wakefields

The integrated fields seen by a test particle traveling on the same, or on a parallel path at a constant distance s behind a point charge Q are called the integrated longitudinal and transverse wakepotentials. They are defined as:

$$\tilde{W}_{\perp}(\Delta r, s) = \frac{1}{Q}\int_0^L \left[E_{\perp}(\Delta r, z, s) + c\hat{z} \times B(\Delta r, z, s)\right] dz$$
$$\tilde{W}_{\parallel}(s) = -\frac{1}{Q}\int_0^L \left[E_z(z, s)\right] dz$$

The transverse and longitudinal kicks felt by a particle, at position z along the bunch, due to all leading particles ($\forall z' : \; z' > z$):

$$\Delta r' = \frac{\Delta P_{\perp}}{P} = \frac{qQL}{Pc}\int_{-\infty}^{z} W_{\perp}(\Delta r(z'), z - z')\,\rho(z')\,dz'$$
$$\Delta P_{\parallel} = \frac{qQL}{c}\int_{-\infty}^{z} W_{\parallel}(z - z')\,\rho(z')\,dz'$$

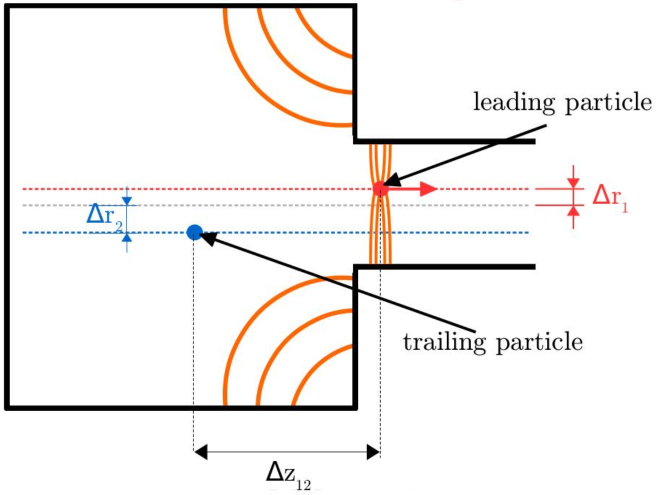

Figure: Scheme of the two-particle model.

with:

- $\rho(z')$ normalized line charge density of the bunch, such that $\int_{-\infty}^{\infty} \rho(z')\,dz' = 1$
- $\Delta r(z')$ transverse radial position of the leading particles as a function of their position z' along the bunch [mm]
- Q total charge of the bunch [C]
- q particle's charge [e]
- P particle's momentum [eV/c]
- $\Delta r'$ radial kick [rad]
- ΔP momentum loss [eV]

Impact of staic and dynamic errors in ATF2: Simulation conditions (1/2)

Simulated errors:

Static errors:
- Misalignement of quadrupoles, sextupoles and BPMs of 100 um RMS.

- Strength error of quadrupoles and sextupoles of 0.1% RMS.

- Roll error for quadrupoles and sextupoles of 200 urad RMS.

Dynamic errors:
- Incoming pos./ang. jitter of $[0.1\sigma_{y/y'} \ - \ 1.0\sigma_{y/y'}]$

Corrections applied:

- One-to-one
- DFS
- WFS
- Knobs $(\underbrace{\text{Y, YP D XP}}_{\text{First order}} \ \underbrace{\text{XP.*XP XP.*YP XP.*D}}_{\text{Second order}})$

Simulation procedure:

Tracking 200 bunches per machine from the ATF extraction line to the IP.

100 machines with the previously cited static imperfections.

Apply the cited corrections and the knobs on the distribution at the IP.

Tracking code used: PLACET

Impact of staic and dynamic errors in ATF2: Simulation conditions (2/2)

Wakefield sources: Cavity BPMs, bellows and flanges (wakepotentials calcultated with GdfidL).[3][4][5]

Position of wakefield sources

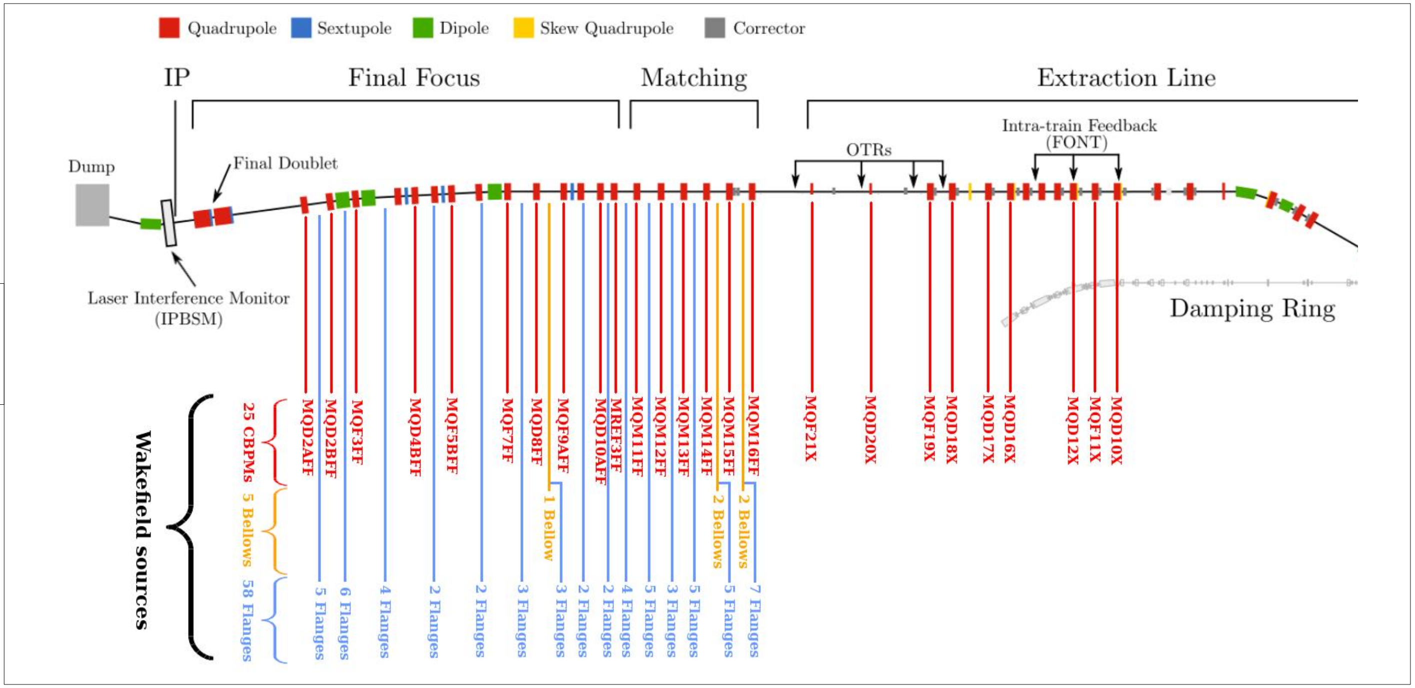

Wakefield sources wakepotentials (V/pC/mm)

Cavity BPM

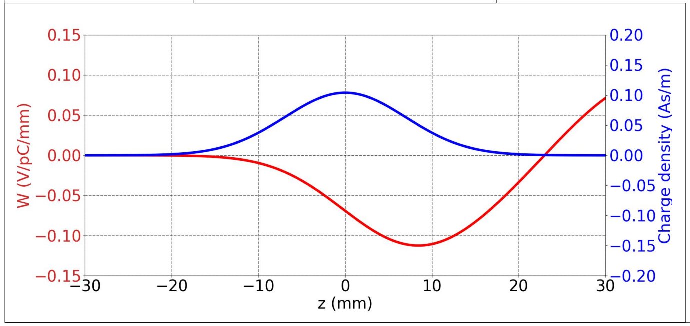

Bellows

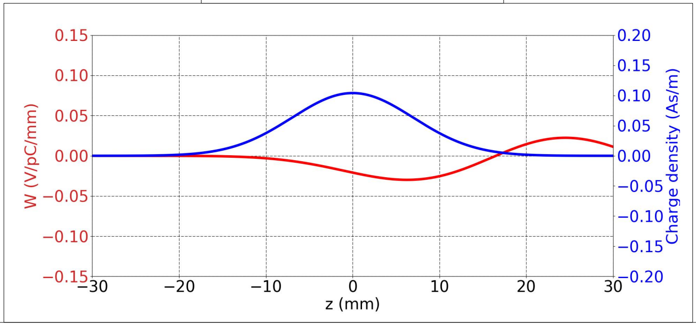

Flange

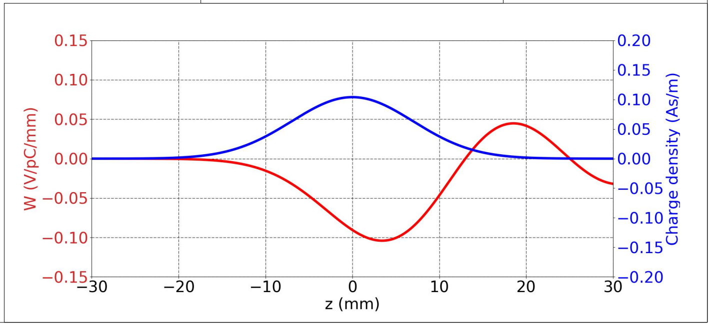

Intensity-dependent effects in ATF2
Measurements

Comparison simulations/measurements

Comparison intensity-dependent effects
Simulations/Measurements

Good agreement between measurements and simulations for the intensity-dependent effects.

Simulations:

Static errors:

- Misalignement of quadrupoles, sextupoles and BPMs of 100 um RMS.
- Strength error of quadrupoles and sextupoles of 0.1% RMS.
- Roll error for quadrupoles and sextupoles of 200 urad RMS.

Dynamic errors:

- Incoming pos. & ang. jitter of $1.0\sigma_y$ and $1.0\sigma_{y'}$ respectively.

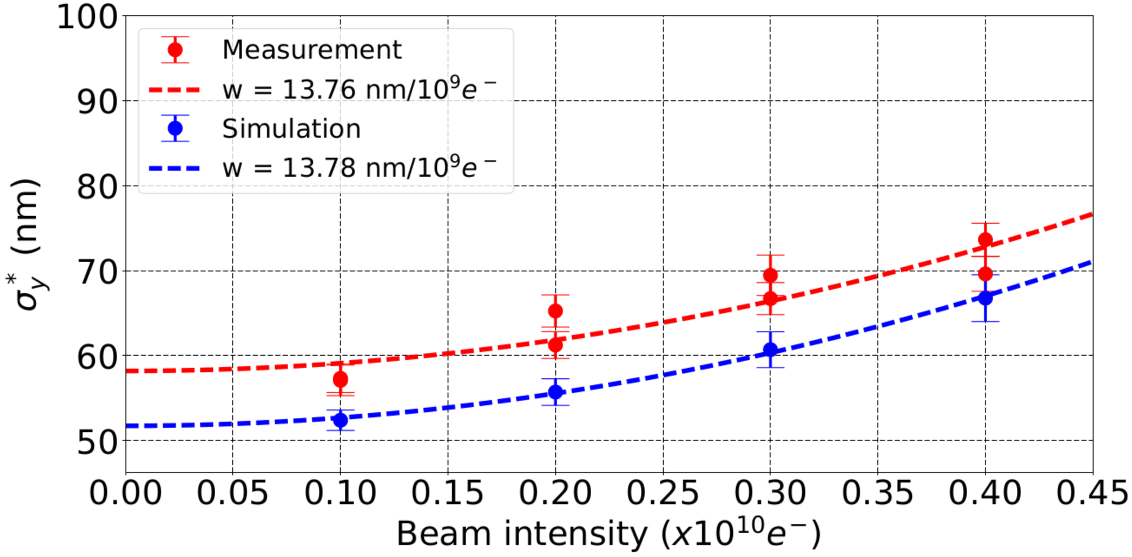

Figure: Comparison between measurements and simulations of the vertical beam size at the IP (σ_y^*) vs. the beam intensity and the intensity-dependent parameter w.

Measurements:

Done on 03/02/2016 (Intensity_fringe_160203_193347)

Case	**w [nm/10^9 e^-]**	**Beam intensity [e^-]**	**$\overline{\sigma_y^*}$ [nm]**
Meas	13.8 ± 1.6	0.1×10^{10}	57.0 ± 1.7
		0.2×10^{10}	63.0 ± 1.7
		0.3×10^{10}	68.0 ± 2.1
		0.4×10^{10}	72.0 ± 2.0
Sim	13.8 ± 0.3	0.1×10^{10}	52.0 ± 1.2
		0.2×10^{10}	56.0 ± 1.6
		0.3×10^{10}	61.0 ± 2.1
		0.4×10^{10}	67.0 ± 2.8

Phys. Rev. Accel. Beams 23, 121004, (2020)

Simulations of the impact of short-range wakefields in the ILC

Impact of corrections and intensity-dependent effects

The ILC Beam Delivery System (BDS)

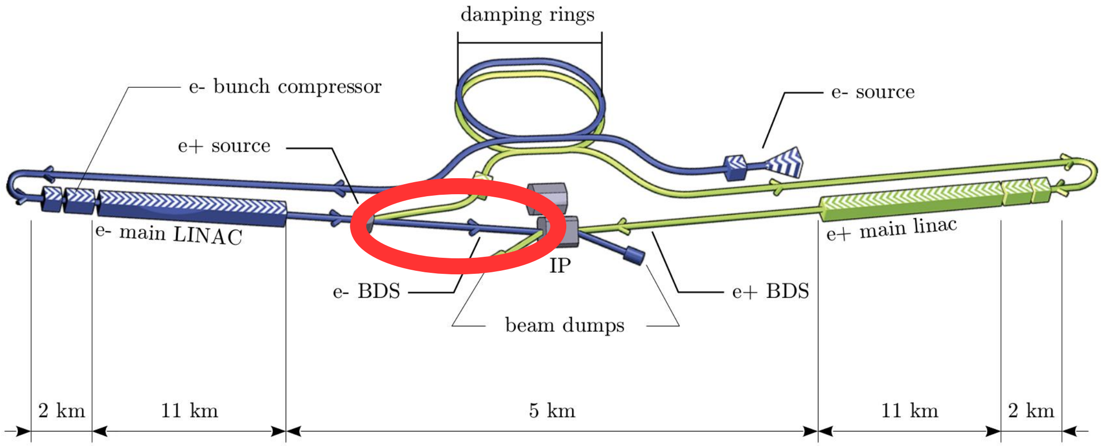

Table: ILC 250 GeV beam parameters.

Parameter	**Symbol**	**Value**
Centre-of-mass energy	E_{CM}	250 GeV
Length of the BDS	L_{BDS}	2254 m
Number of bunches	n_b	1312
Bunch population	N	2.0×10^{10} e^-
RMS bunch length	σ_z	0.3 mm
Bunch separation	Δt_b	554 ns
IP RMS beam sizes	σ_x^*/σ_y^*	516/7.7 nm

Table: 500 GeV ILC beam parameters.

Parameter	**Symbol**	**Value**
Centre-of-mass energy	E_{CM}	500 GeV
Length of the BDS	L_{BDS}	2254 m
Number of bunches	n_b	1312
Bunch population	N	2.0×10^{10} e^-
RMS bunch length	σ_z	0.3 mm
Bunch separation	Δt_b	554 ns
IP RMS beam sizes	σ_x^*/σ_y^*	474/5.9 nm

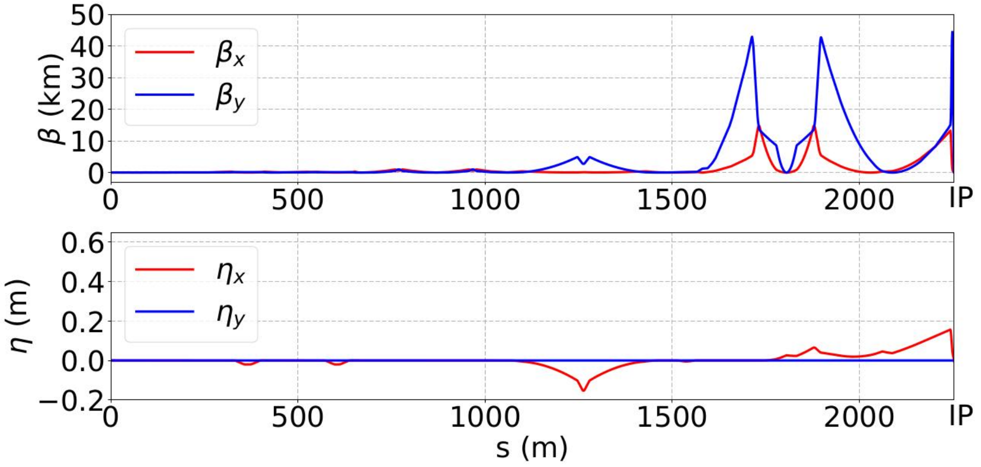

Figure: The ILC BDS 500 GeV Twiss parameters calculated with PLACET

The ILC Beam Delivery System (BDS)

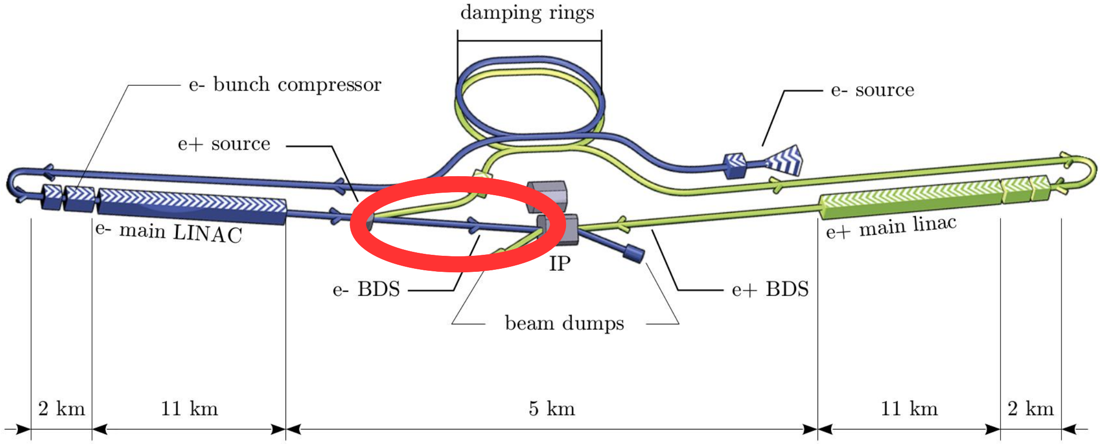

Table: ILC 250 GeV beam parameters.

Parameter	**Symbol**	**Value**
Centre-of-mass energy	E_{CM}	250 GeV
Length of the BDS	L_{BDS}	2254 m
Number of bunches	n_b	1312
Bunch population	N	2.0×10^{10} e^-
RMS bunch length	σ_z	0.3 mm
Bunch separation	Δt_b	554 ns
IP RMS beam sizes	σ_x^*/σ_y^*	516/7.7 nm

Table: 500 GeV ILC beam parameters.

Parameter	**Symbol**	**Value**
Centre-of-mass energy	E_{CM}	500 GeV
Length of the BDS	L_{BDS}	2254 m
Number of bunches	n_b	1312
Bunch population	N	2.0×10^{10} e^-
RMS bunch length	σ_z	0.3 mm
Bunch separation	Δt_b	554 ns
IP RMS beam sizes	σ_x^*/σ_y^*	474/5.9 nm

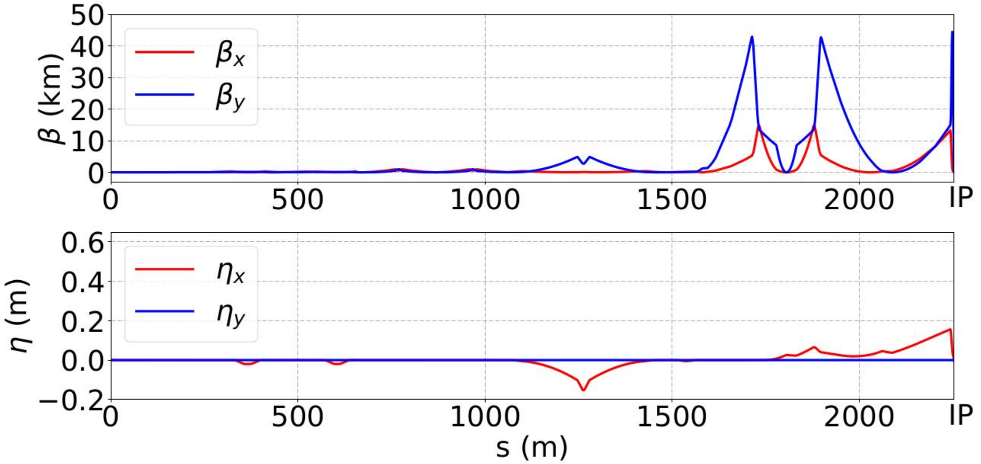

Figure: The ILC BDS 500 GeV Twiss parameters calculated with PLACET

Impact of corrections in ILC
Simulation conditions (1/2)

Simulated errors:

- Static errors:

  - Misalignement of quadrupoles, sextupoles and BPMs of 50 µm RMS.

  - Strength error of quadrupoles and sextupoles of 0.1% RMS.

  - Roll error for quadrupoles and sextupoles of 200 µrad RMS.

Corrections applied:

- One-to-one
- DFS
- WFS
- Knobs ($\underbrace{\text{Y, YP D XP}}_{\text{First order}}$ $\underbrace{\text{XP.*XP XP.*YP XP.*D}}_{\text{Second order}}$)

Simulation procedure:

- 100 machines with the previously cited static imperfections.
- Apply the cited corrections and the knobs on the distribution at the IP.
- Measure the vertical beam size at the IP.

Impact of corrections in ILC
Simulation conditions (2/2)

Wakefield sources: C-band cavity BPMs (C-BPMs), wakepotentials calcultated with GdfidL.

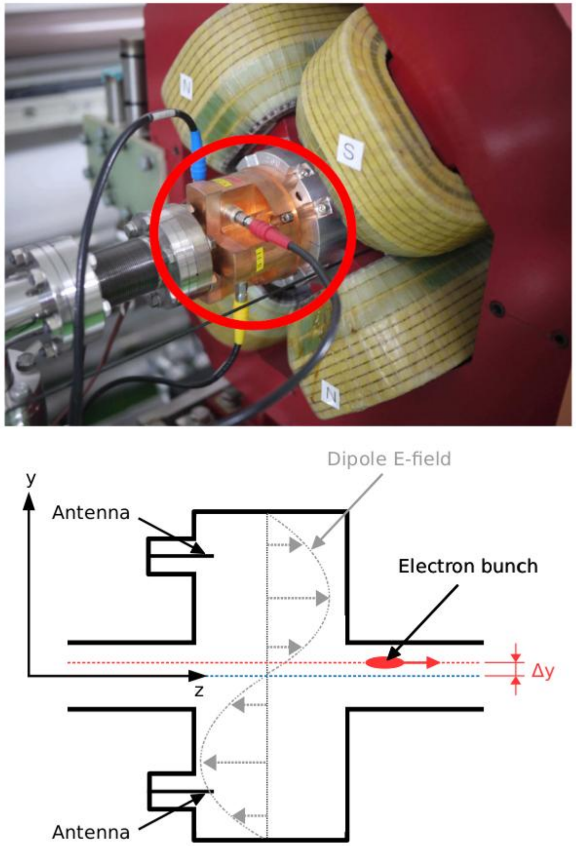

Figure: Picture of an ATF2 C-BPM (top) and schematic of a C-BPM (bottom).

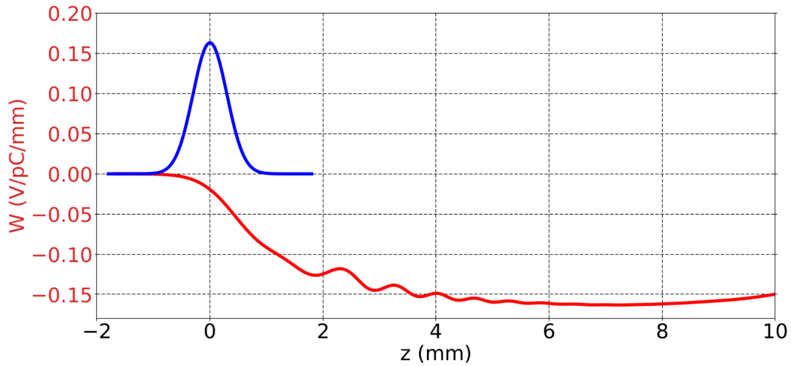

Figure : Transverse wakepotential in V/pC/mm of the ILC C-BPM, calculated with GdfidL for a vertical offset of 1 mm, Gaussian bunch length of 0.3 mm and 1 pC charge (in red). For reference, the distribution of the electrons in one bunch is shown (in blue).

Table: Positions of ILC BDS C-BPMs.

BPM #	s (m)	BPM #	s (m)	BPM #	s (m)	BPM #	s (m)
1	0.5	27	671.2	53	1247.1	79	1731.2
2	16.0	28	674.4	54	1261.1	80	1731.7
3	31.5	29	704.3	55	1265.1	81	1733.0
4	47.0	30	760.4	56	1279.1	82	1778.8
5	58.1	31	766.7	57	1429.0	83	1805.7
6	69.1	32	769.8	58	1468.2	84	1832.6
7	80.0	33	773.0	59	1481.0	85	1878.4
8	91.1	34	779.3	60	1495.0	86	1880.2
9	106.6	35	835.4	61	1509.0	87	1880.7
10	122.1	36	865.3	62	1510.7	88	1882.0
11	137.6	37	868.5	63	1537.9	89	1892.2
12	157.3	38	871.6	64	1565.1	90	1894.1
13	160.6	39	901.5	65	1566.7	91	1895.9
14	172.8	40	957.6	66	1580.7	92	1896.4
15	190.0	41	963.9	67	1594.7	93	1897.7
16	191.0	42	967.1	68	1607.9	94	2034.8
17	207.2	43	970.2	69	1614.9	95	2061.7
18	224.4	44	976.5	70	1654.4	96	2088.6
19	225.4	45	1013.8	71	1659.4	97	2242.8
20	241.6	46	1054.0	72	1697.6	98	2243.3
21	258.8	47	1058.0	73	1713.7	99	2243.4
22	259.8	48	1097.2	74	1715.5	100	2244.7
23	323.0	49	1135.4	75	1717.3	101	2247.4
24	326.5	50	1160.0	76	1719.2	102	2247.7
25	367.2	51	1184.6	77	1719.2	103	2247.7
26	466.5	52	1209.2	78	1729.4	104	2248.9

The short-range wakefield sources taken into account are the 104 ILC C-BPMs.

Impact of corrections in the ILC 250 and 500 GeV BDS

500 GeV - 1 machine

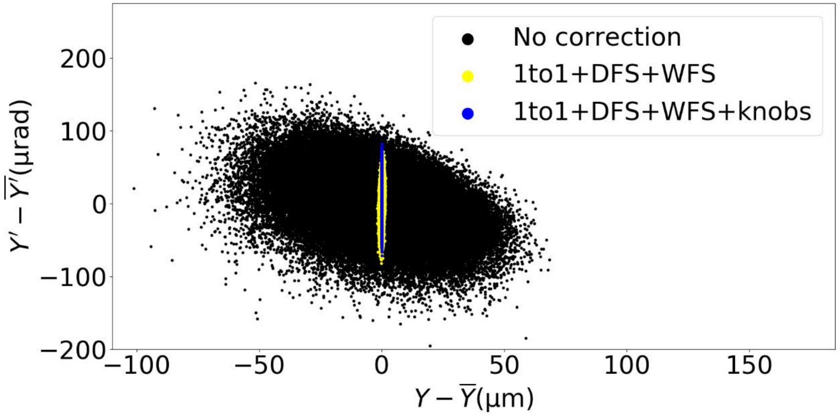

Figure : Centered vertical phase space at the 500 GeV ILC BDS IP, $Y' - \overline{Y'}$ vs. $Y - \overline{Y}$, for 3 cases: no correction, One-to-one steering, DFS, WFS and One-to-one steering, DFS, WFS and knobs, calculated with PLACET with wakefields.

500 GeV - 100 machines

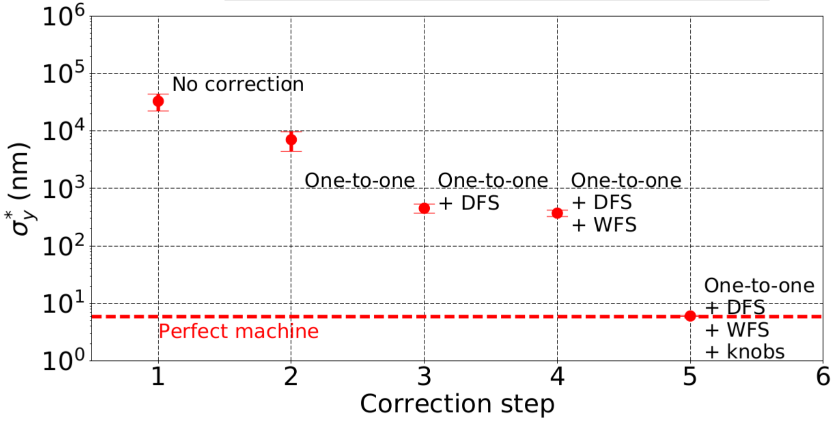

Figure : Average vertical beam size at the 500 GeV ILC IP (σ_y^*) vs. correction step: One-to-one, DFS, WFS corrections and IP tuning knobs. The red dashed line show the vertical beam size at the IP for a perfect machine, 5.9 nm.

250 GeV - 100 machines

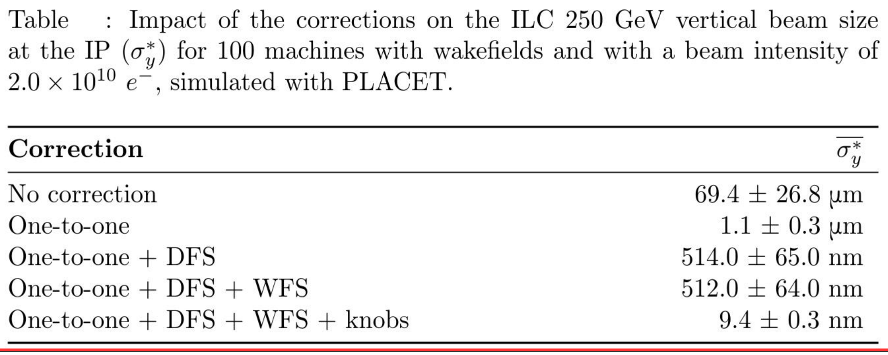

Table : Impact of the corrections on the ILC 250 GeV vertical beam size at the IP (σ_y^*) for 100 machines with wakefields and with a beam intensity of 2.0×10^{10} e^-, simulated with PLACET.

Correction	σ_y^*
No correction	69.4 ± 26.8 µm
One-to-one	1.1 ± 0.3 µm
One-to-one + DFS	514.0 ± 65.0 nm
One-to-one + DFS + WFS	512.0 ± 64.0 nm
One-to-one + DFS + WFS + knobs	9.4 ± 0.3 nm

500 GeV - 100 machines

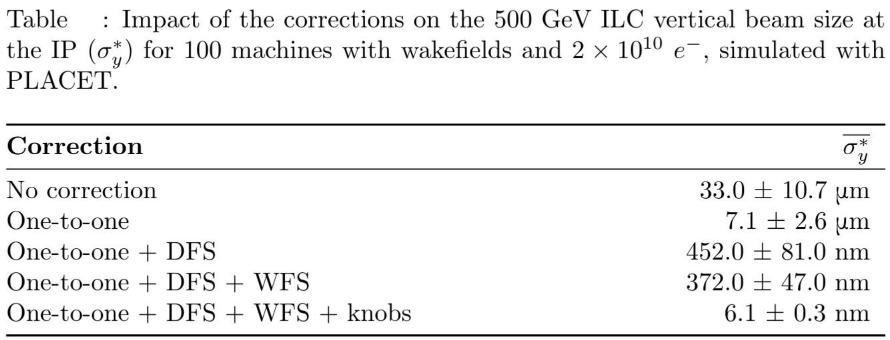

Table : Impact of the corrections on the 500 GeV ILC vertical beam size at the IP (σ_y^*) for 100 machines with wakefields and 2×10^{10} e^-, simulated with PLACET.

Correction	σ_y^*
No correction	33.0 ± 10.7 µm
One-to-one	7.1 ± 2.6 µm
One-to-one + DFS	452.0 ± 81.0 nm
One-to-one + DFS + WFS	372.0 ± 47.0 nm
One-to-one + DFS + WFS + knobs	6.1 ± 0.3 nm

Orbit corrections and knobs reduce the beam size by a factor 5400 for the 500 GeV case.

Impact of short-range wakefields in the 250 and 500 GeV BDS

250 GeV

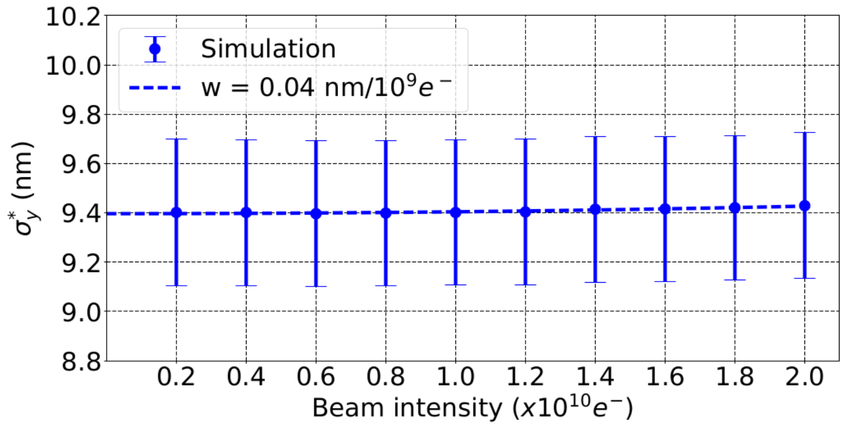

Figure : Vertical IP beam size σ_y^* vs. beam intensity in the 250 GeV BDS, calculated with PLACET with wakefields.

500 GeV

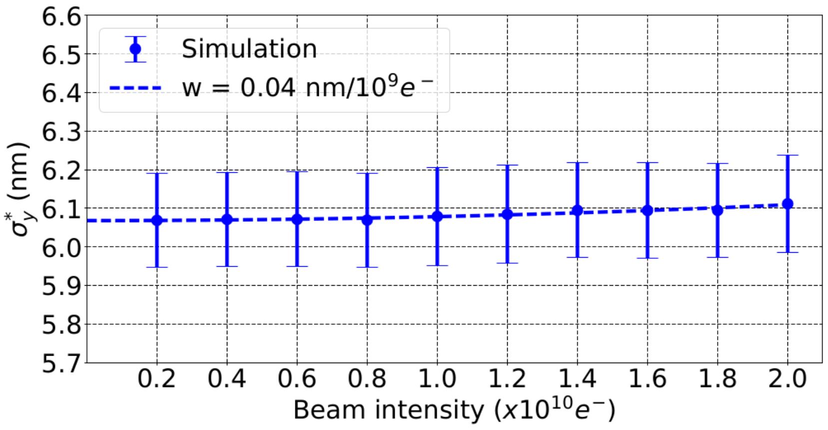

Figure : Vertical IP beam size σ_y^* vs. beam intensity in the 500 GeV BDS, calculated with PLACET with wakefields.

250 GeV

Table : Intensity-dependent effects due to wakefields on the vertical IP beam size σ_y^* in the 250 GeV ILC BDS, calculated with PLACET with wakefields.

Beam intensity	$\overline{\sigma_y^*}$ **(nm)**	w (nm/10^9 e^-)
0.2×10^{10} e^-	9.4 ± 0.3	0.04
2.0×10^{10} e^-	9.4 ± 0.3	

500 GeV

Table : Intensity-dependent effects due to wakefields on the vertical IP beam size σ_y^* in the 500 GeV BDS, calculated with PLACET with wakefields.

Beam intensity	$\overline{\sigma_y^*}$ **(nm)**	w (nm/10^9 e^-)
0.2×10^{10} e^-	6.1 ± 0.3	0.04
2.0×10^{10} e^-	6.1 ± 0.3	

Short-range wakefield effects are negligible in both 250 and 500 GeV BDS

$$w[nm/10^9 e]=\frac{(\sqrt{\sigma_{y,q}^2-\sigma_{y,0}^2})}{q}$$

Simulations of the impact of long-range wakefields

In the 250 and 500 GeV ILC BDS

Long-range wakefields in the ILC BDS
Resistive walls wakefield

- Electrons going through the pipe interacts with the surrounding structure and generates a wake field.
- This wake field produces a transverse kick for the following bunches.
- The following model is used for the transverse wake function [6]:

$$W(z)=\frac{c}{\pi b^3}\sqrt{\left(\frac{Z_0}{\sigma_r \pi z}\right)}L$$

With b the radius of the beam pipe, Z_0 the impedance of the vacuum, σ_r the conductivity of the pipe and L the length of the beam line element.

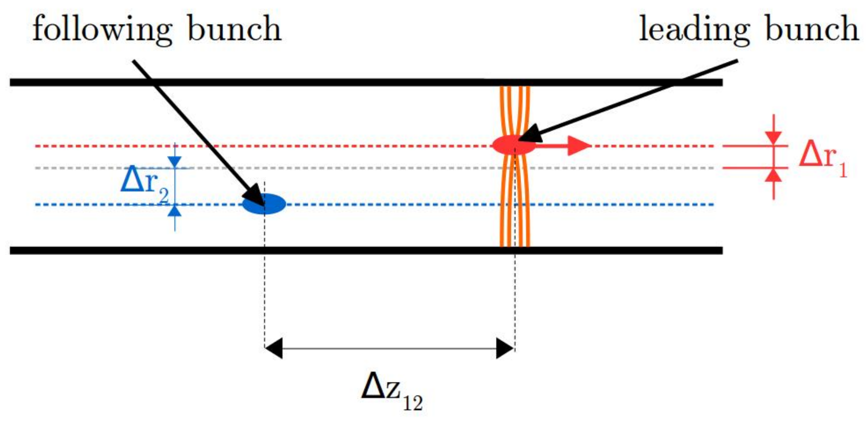

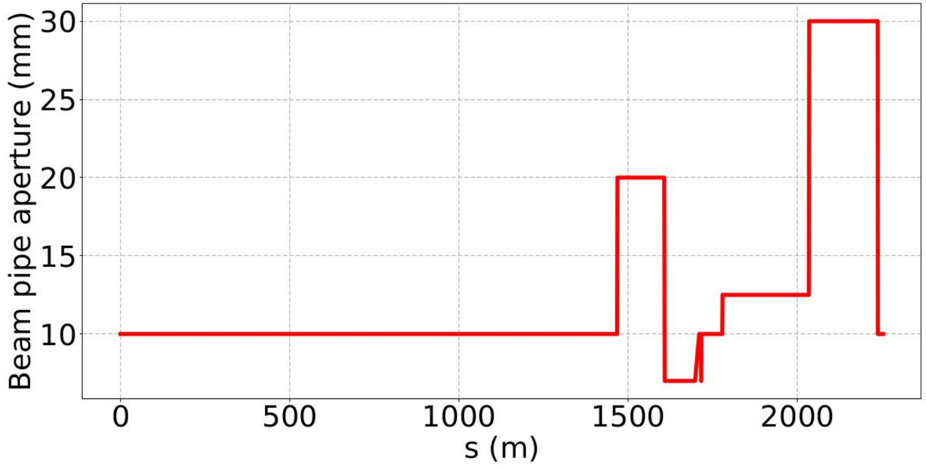

Figure: The ILC BDS beam aperture profile vs. s.

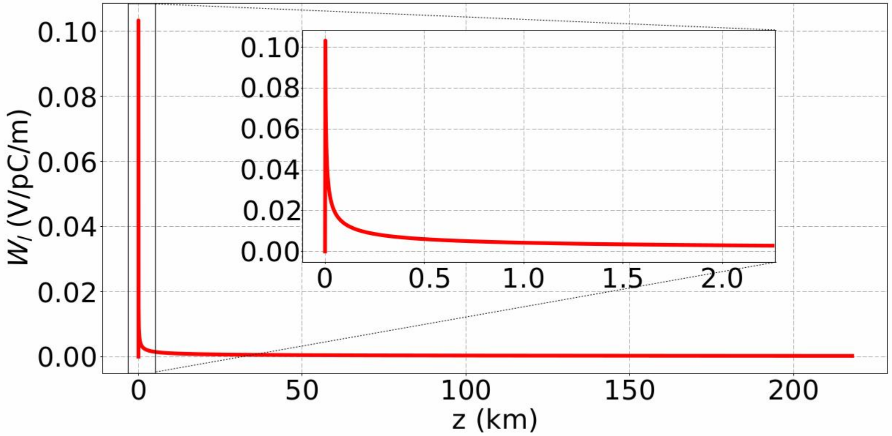

Figure : The ILC resistive walls wakepotential for a copper beam pipe with a constant radius of 10 mm for the length of a train (~218 km). The zoom shows the wakepotential for the length of the ILC BDS (~ 2254 m).

Impact of long-range wakefields in the 250 GeV ILC BDS for a constant offset

Simulation procedure:

- A train of 1312 bunches is injected at the entrance of the BDS.
- Each bunch is made of one macro-particle.
- Incoming position and angle offset of the train to study the impact of long-range wakefields. Amplitude of the incoming offsets: 0.01, 0.05, 0.1σ_y or $\sigma_{y'}$ with σ_y and $\sigma_{y'}$ the beam size and the beam divergence at the entrance of the BDS.

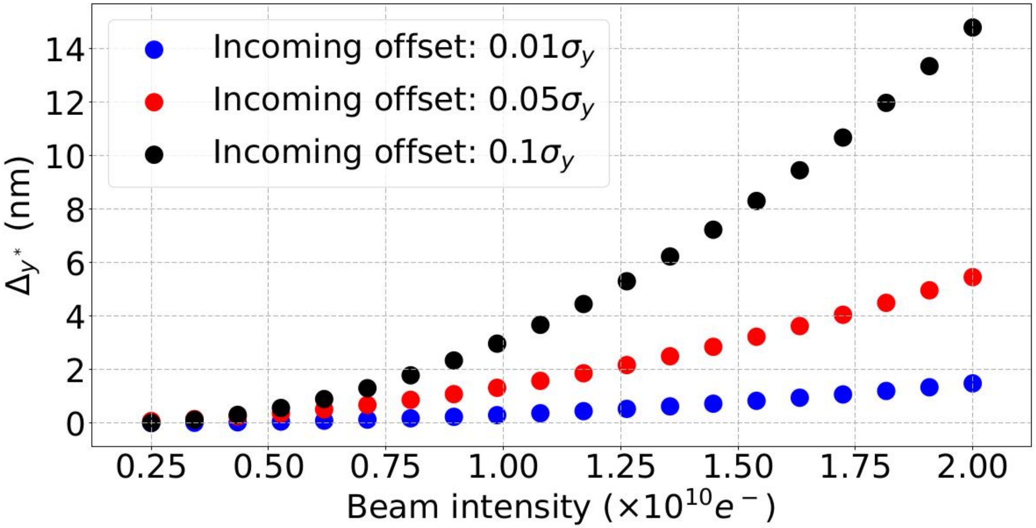

Figure : Vertical orbit deflection at the IP between the first and last bunch of a train Δy^* vs. beam intensity for three incoming constant position offsets of the train of bunches in the 250 GeV ILC BDS: $0.01\sigma_y$, $0.05\sigma_y$ and $0.1\sigma_y$, calculated with PLACET with resistive wall effects included.

$\sigma_y = 0.82\,\mu m$

$\sigma_{y'} = 0.097\,\mu rad$

Impact of long-range wakefields in the 250 GeV ILC BDS for a constant offset

- Study of the impact of long-range wakefields for a train injected in the BDS with a constant vertical position and an angle offset of $0.01\sigma_y$ and $0.01\sigma_{y'}$ respectively on the vertical orbit deflection at the IP normalized by the IP beam size, Δ_y/σ_y^* (left).
- Same study was done for both vertical and horizontal incoming offsets (right).

$$\sigma_{y'}=0.097\,\mu rad \qquad \sigma_y=0.82\,\mu m \qquad \sigma_y^*=7.7\,nm$$

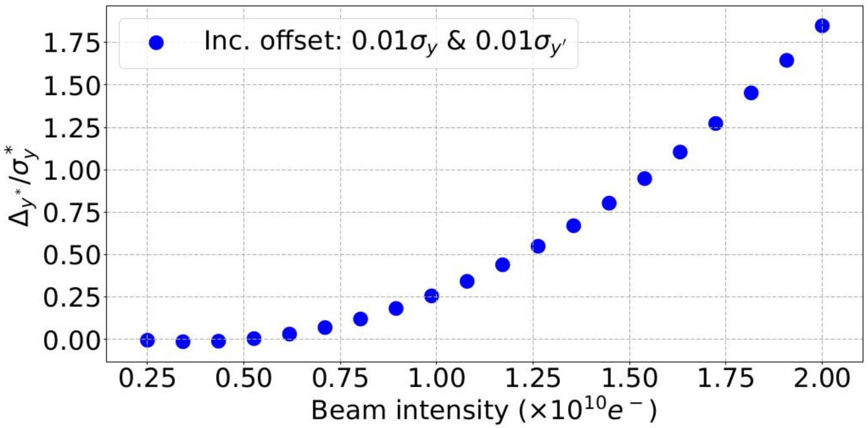

Figure : Vertical orbit deflection at the IP between the first and last bunch of a train normalised by the IP vertical beam size ($\Delta y^*/\sigma_y^*$) vs. beam intensity for a train with incoming constant position and angle offsets of respectively $0.01\sigma_y$ and $0.01\sigma_{y'}$ in the 250 GeV ILC BDS, calculated with PLACET with resistive wall effects included.

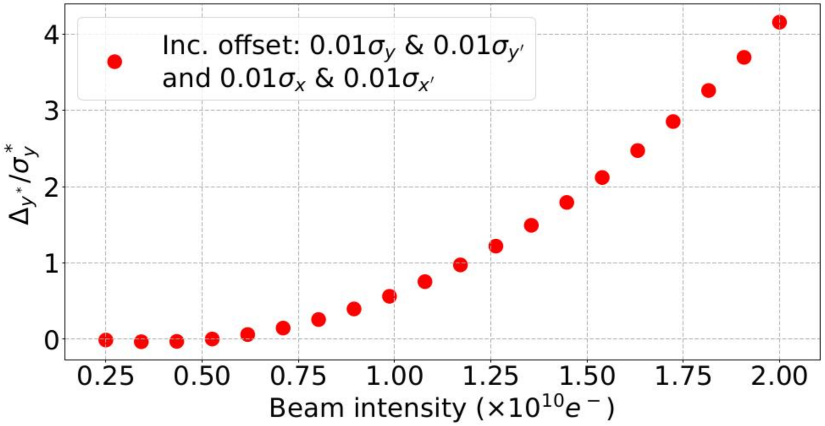

Figure : Vertical orbit deflection at the IP between the first and last bunch of a train normalised by the IP vertical beam size ($\Delta y^*/\sigma_y^*$) vs. beam intensity for a train with incoming constant horizontal position and angle offsets of respectively $0.01\sigma_x$ and $0.01\sigma_{x'}$ and vertical incoming position and angle offsets of respectively $0.01\sigma_y$ and $0.01\sigma_{y'}$ in the 250 GeV ILC BDS, calculated with PLACET with resistive wall effects included.

Constant incoming offsets lead to a significant effect of long-range wakefields

Impact of long-range wakefields in the 250 GeV ILC BDS for a random offset

- Study of the impact of long-range wakefields for a train injected in the BDS with a random horizontal and vertical position and an angle offsets.
- The distribution of random incoming position and angle offset is a normal distribution with a zero mean and variance of 2.6x10^{-4}, leading to a $+/-$ 5% incoming vertical and horizontal angle and position offsets.

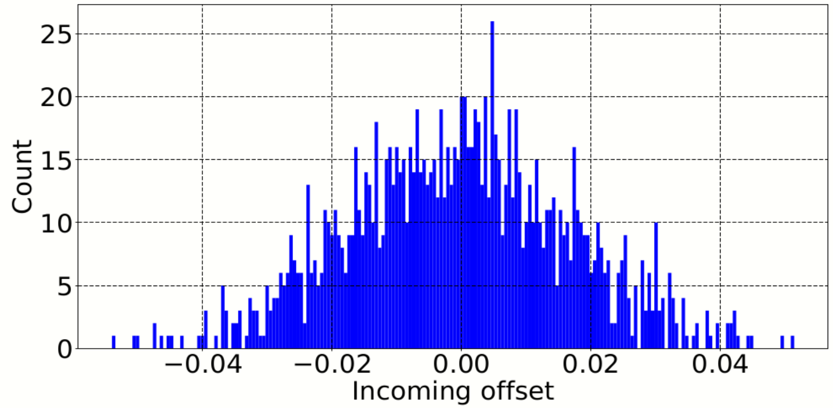

Figure : Distribution of incoming position and angle offsets from -0.05$\sigma_{x,y}$ to 0.05$\sigma_{x,y}$.

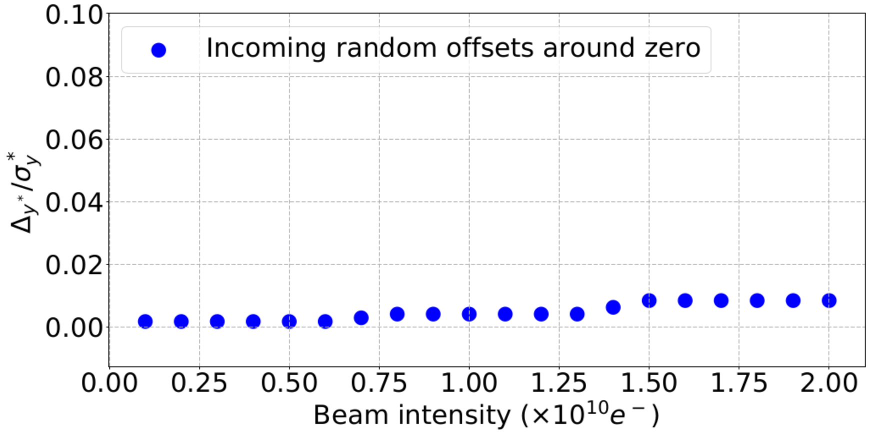

Figure : Vertical orbit deflection at the IP between the first and last bunch of a train normalised by the IP vertical beam size ($\Delta y^*/\sigma_y^*$) vs. beam intensity for a train with a random and around zero incoming vertical and horizontal position and angle offsets of between -0.05 and 0.05 σ in the 250 GeV ILC BDS, calculated with PLACET with resistive wall effects included.

Random incoming offsets lead to a negligible effect of long-range wakefields

Impact of long-range wakefields in the 250 and 500 GeV ILC BDS Luminosity

- Study of the impact of luminosity degradation due to the vertical orbit deflection at the IP with Guinea-Pig, a code simulating the impact of beam-beam effects on luminosity and background [7].

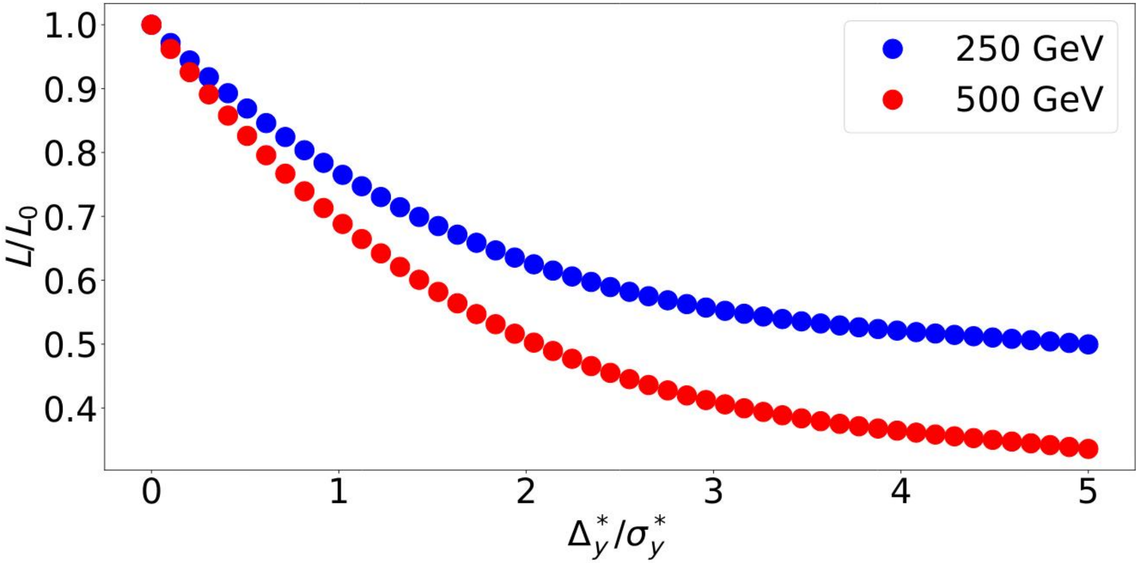

FIG. 250 and 500 GeV ILC luminosity degradation vs. relative vertical offset of the colliding beams.

$$L = f_{coll} \frac{n_1 n_2}{4\pi\sigma_x^*\sigma_y^*} F$$

Impact of long-range wakefields in the 250 and 500 GeV ILC BDS Summary

250 GeV

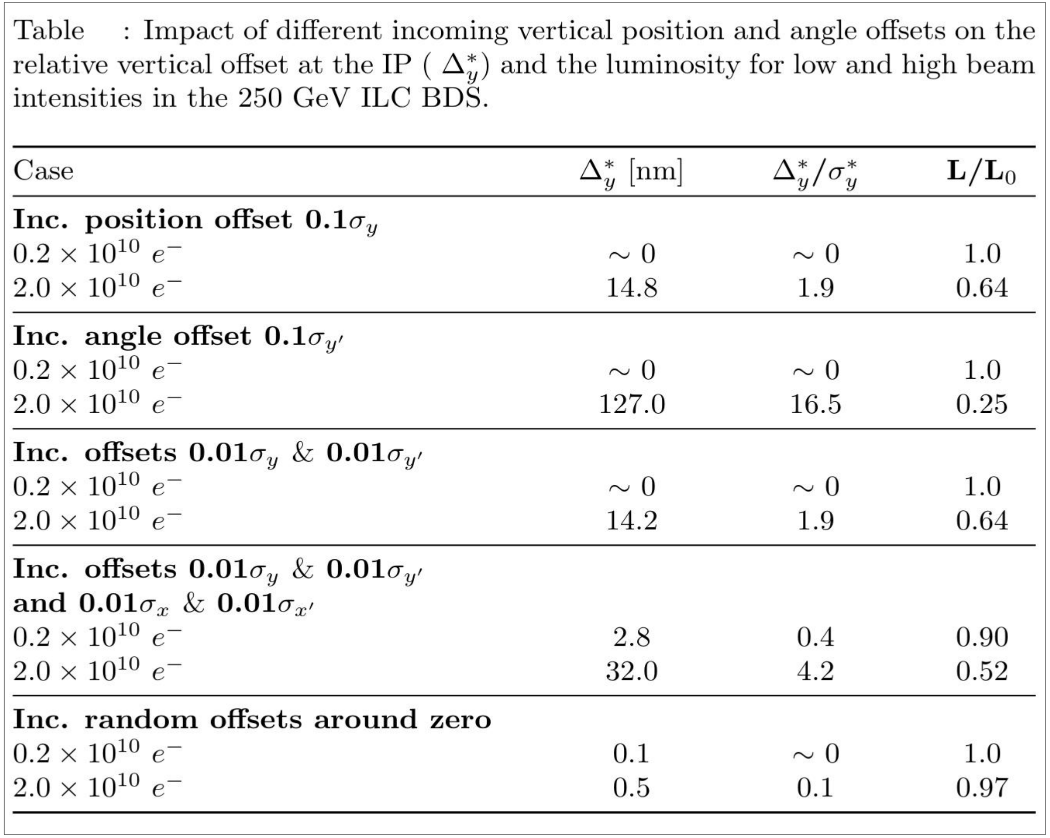

Table : Impact of different incoming vertical position and angle offsets on the relative vertical offset at the IP (Δ_y^*) and the luminosity for low and high beam intensities in the 250 GeV ILC BDS.

Case	Δ_y^* [nm]	Δ_y^*/σ_y^*	$\mathbf{L/L_0}$
Inc. position offset 0.1σ_y			
0.2×10^{10} e^-	~ 0	~ 0	1.0
2.0×10^{10} e^-	14.8	1.9	0.64
Inc. angle offset 0.1$\sigma_{y'}$			
0.2×10^{10} e^-	~ 0	~ 0	1.0
2.0×10^{10} e^-	127.0	16.5	0.25
Inc. offsets 0.01σ_y & 0.01$\sigma_{y'}$			
0.2×10^{10} e^-	~ 0	~ 0	1.0
2.0×10^{10} e^-	14.2	1.9	0.64
Inc. offsets 0.01σ_y & 0.01$\sigma_{y'}$ and 0.01σ_x & 0.01$\sigma_{x'}$			
0.2×10^{10} e^-	2.8	0.4	0.90
2.0×10^{10} e^-	32.0	4.2	0.52
Inc. random offsets around zero			
0.2×10^{10} e^-	0.1	~ 0	1.0
2.0×10^{10} e^-	0.5	0.1	0.97

500 GeV

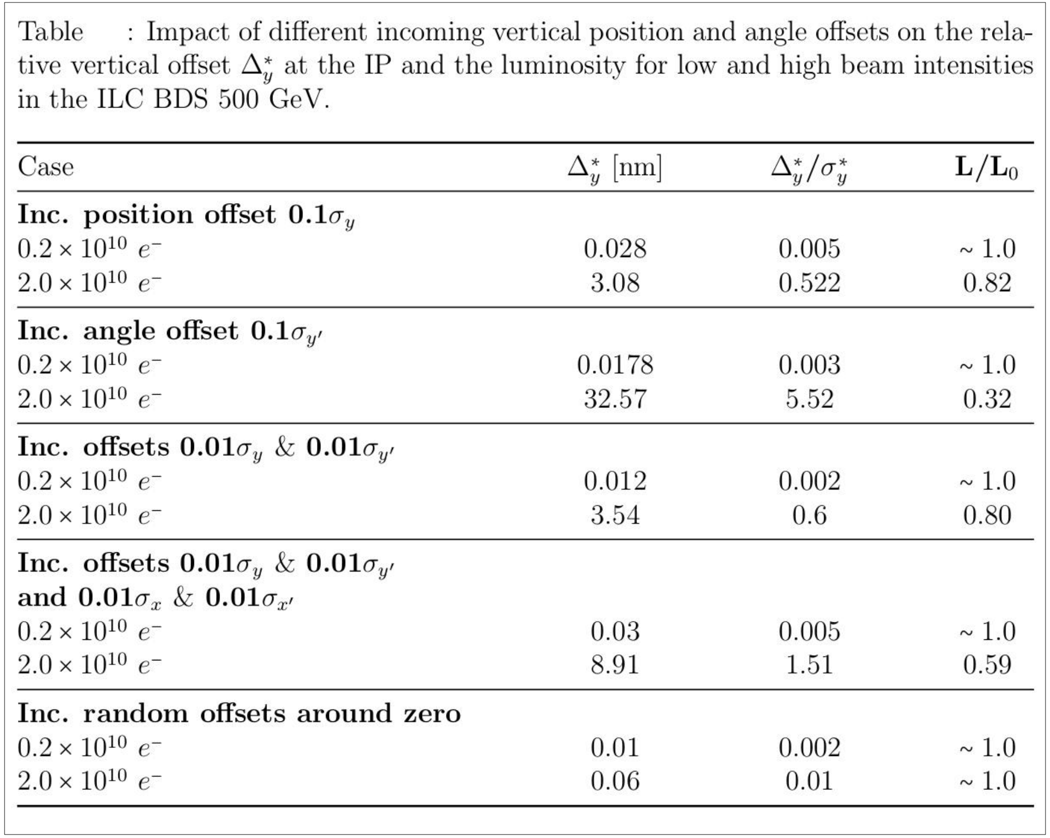

Table : Impact of different incoming vertical position and angle offsets on the relative vertical offset Δ_y^* at the IP and the luminosity for low and high beam intensities in the ILC BDS 500 GeV.

Case	Δ_y^* [nm]	Δ_y^*/σ_y^*	$\mathbf{L/L_0}$
Inc. position offset 0.1σ_y			
0.2×10^{10} e^-	0.028	0.005	~ 1.0
2.0×10^{10} e^-	3.08	0.522	0.82
Inc. angle offset 0.1$\sigma_{y'}$			
0.2×10^{10} e^-	0.0178	0.003	~ 1.0
2.0×10^{10} e^-	32.57	5.52	0.32
Inc. offsets 0.01σ_y & 0.01$\sigma_{y'}$			
0.2×10^{10} e^-	0.012	0.002	~ 1.0
2.0×10^{10} e^-	3.54	0.6	0.80
Inc. offsets 0.01σ_y & 0.01$\sigma_{y'}$ and 0.01σ_x & 0.01$\sigma_{x'}$			
0.2×10^{10} e^-	0.03	0.005	~ 1.0
2.0×10^{10} e^-	8.91	1.51	0.59
Inc. random offsets around zero			
0.2×10^{10} e^-	0.01	0.002	~ 1.0
2.0×10^{10} e^-	0.06	0.01	~ 1.0

Long-range wakefields have a significant impact in the 250 and 500 GeV ILC BDS. An intra-train feedback system would be necessary in order to achieve the luminosity goals.

Simulations of the impact of short-range wakefields in CLIC

Impact of corrections and intensity-dependent effects

The CLIC Beam Delivery System (BDS)

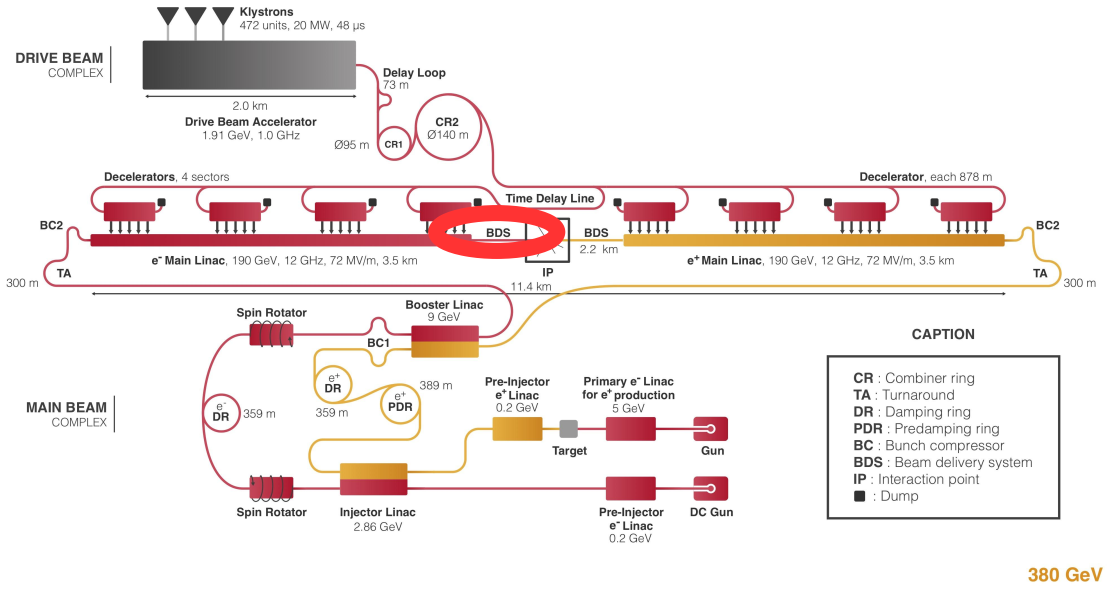

Table: CLIC 380 GeV beam parameters.

Parameter	Symbol	Value
Centre-of-mass energy	E_{CM}	380 GeV
Length of the BDS	L_{BDS}	1949 m
Number of bunches	n_b	352
Bunch population	N	5.2 $\times 10^9$ e^-
RMS bunch length	σ_z	70 μm
Bunch separation	Δt_b	0.5 ns
IP RMS beam sizes	σ_x^*/σ_y^*	149/2.9 nm

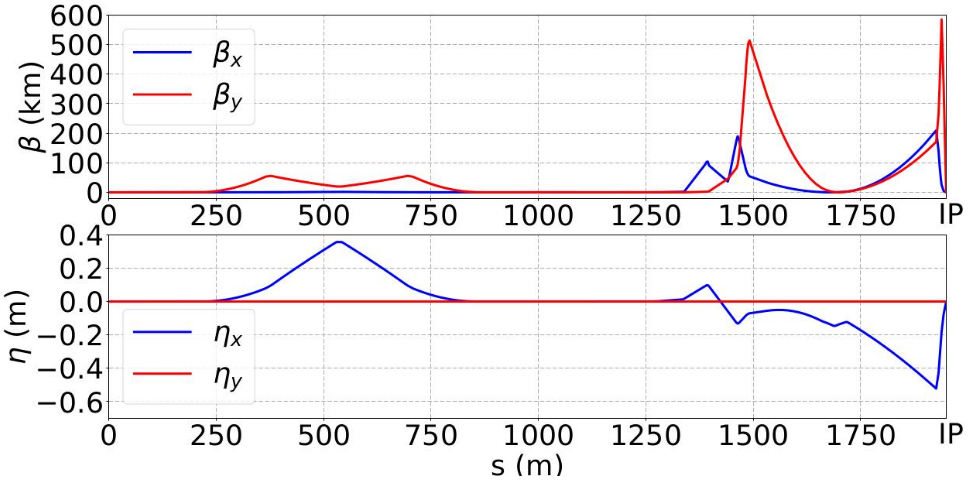

Figure: CLIC BDS 380 GeV Twiss parameters calculated with PLACET.

Impact of corrections in CLIC
Simulation conditions (1/2)

Simulated errors:

- Static errors:

  - Misalignement of quadrupoles, sextupoles and BPMs of 50 µm RMS.

  - Strength error of quadrupoles and sextupoles of 0.1% RMS.

  - Roll error for quadrupoles and sextupoles of 200 µrad RMS.

Corrections applied:

- One-to-one
- DFS
- WFS
- Knobs $(\underbrace{\text{Y, YP D XP}}_{\text{First order}}\ \underbrace{\text{XP.*XP XP.*YP XP.*D}}_{\text{Second order}})$

Simulation procedure:

- 100 machines with the previously cited static imperfections.
- Apply the cited corrections and the knobs on the distribution at the IP.
- Measure the vertical beam size at the IP.

Impact of corrections in CLIC
Simulation conditions (2/2)

Wakefield sources: X-band cavity BPMs (C-BPMs), wakepotentials calcultated with GdfidL.

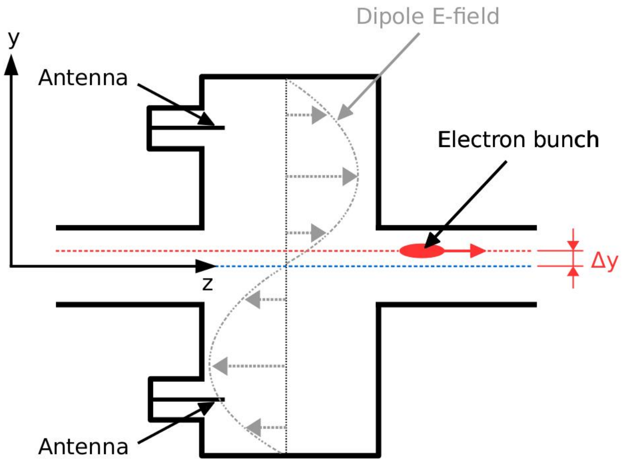

Figure: Schematic of a C-BPM.

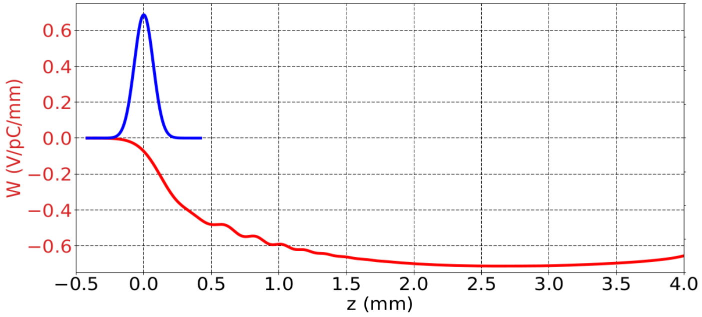

Figure : Transverse wakepotential in V/pC/mm of the CLIC C-BPM, calculated with GdfidL for a vertical offset of 1 mm, Gaussian bunch length of 70 µm and 1 pC charge (in red). For reference, the distribution of the electrons in one bunch is shown (in blue).

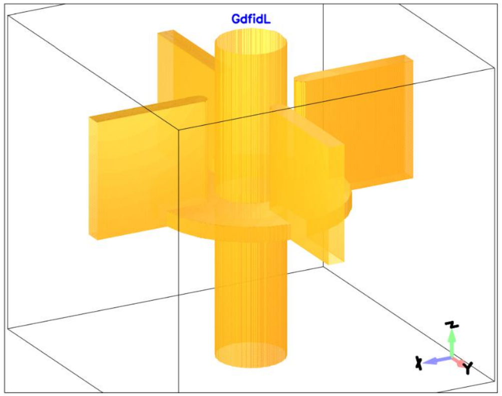

Figure: Geometry of the CLIC C-BPM, generated with GdfidL.

Table: Positions of CLIC 380 GeV BDS C-BPMs.

#	s (m)	#	s (m)	#	s (m)	#	s (m)	#	s (m)
1	0.0	28	158.9	55	868.4	82	971.4	109	1131.2
2	5.5	29	159.4	56	868.9	83	979.8	110	1131.7
3	11.0	30	178.1	57	869.5	84	980.3	111	1140.1
4	16.5	31	178.6	58	870.0	85	998.4	112	1147.0
5	17.0	32	197.2	59	870.6	86	998.9	113	1159.5
6	26.4	33	202.0	60	871.1	87	999.8	114	1172.0
7	36.3	34	205.0	61	871.8	88	1000.3	115	1184.3
8	36.8	35	211.0	62	872.3	89	1018.4	116	1193.0
9	40.3	36	212.3	63	884.4	90	1018.9	117	1205.9
10	40.8	37	363.5	64	884.9	91	1027.3	118	1218.8
11	44.4	38	364.8	65	885.5	92	1027.8	119	1231.2
12	44.9	39	376.0	66	886.0	93	1036.2	120	1246.8
13	48.5	40	377.3	67	886.9	94	1036.7	121	1279.9
14	49.0	41	528.5	68	887.4	95	1054.8	122	1333.9
15	52.5	42	529.8	69	905.5	96	1055.3	123	1337.1
16	53.0	43	541.0	70	906.0	97	1056.2	124	1391.0
17	62.4	44	542.3	71	914.4	98	1056.7	125	1394.2
18	62.9	45	693.5	72	914.9	99	1074.8	126	1460.6
19	72.3	46	694.8	73	923.3	100	1075.3	127	1463.8
20	72.8	47	706.0	74	923.8	101	1083.7	128	1483.6
21	82.2	48	707.3	75	941.9	102	1084.2	129	1488.6
22	101.3	49	858.5	76	942.4	103	1092.6	130	1658.2
23	101.8	50	859.8	77	943.4	104	1093.1	131	1687.4
24	120.5	51	866.1	78	943.9	105	1111.2	132	1716.7
25	121.0	52	866.6	79	961.9	106	1111.7	133	1925.7
26	139.7	53	867.3	80	962.4	107	1112.6	134	1938.4
27	140.2	54	867.8	81	970.9	108	1113.1		

The short-range wakefield sources taken into account are the 134 CLIC C-BPMs.

Impact of corrections
in the CLIC 380 GeV BDS

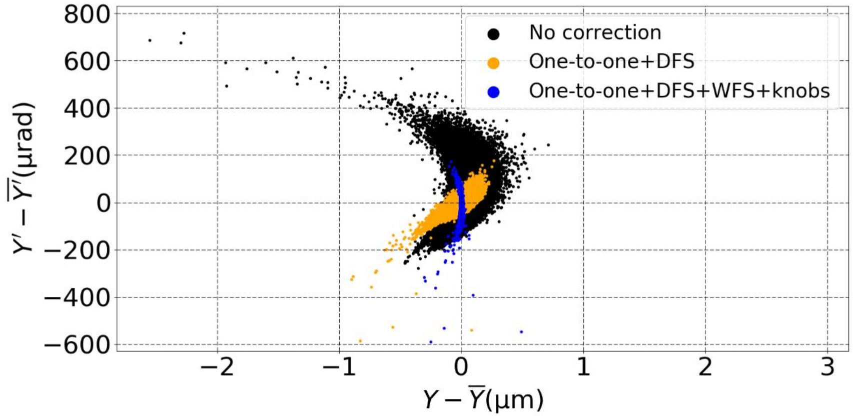

Figure : Centered vertical phase space at the 380 GeV CLIC BDS IP, $Y' - \overline{Y'}$ vs. $Y - \overline{Y}$, for 3 cases: no correction, One-to-one steering, DFS, WFS and One-to-one steering, DFS, WFS and knobs, calculated with PLACET with wakefields.

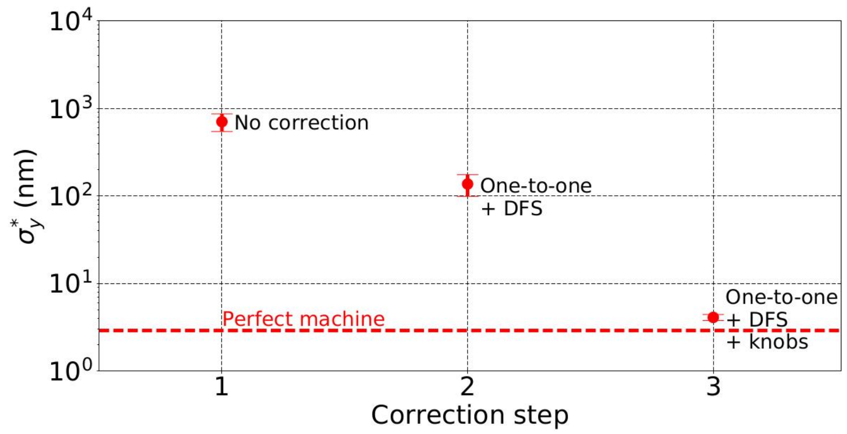

Figure : Average vertical beam size at the 380 GeV CLIC IP (σ_y^*) vs. correction step: One-to-one, DFS, WFS corrections and IP tuning knobs. The red dashed line show the vertical beam size at the IP for a perfect machine, 2.9 nm, calculated with PLACET with wakefields.

Table : Impact of the corrections on the CLIC 380 GeV vertical beam size at the IP (σ_y^*) for 100 machines with wakefields and with a beam intensity of 5.2×10^9 e^-, calculated with PLACET with wakefields.

Correction	$\overline{\sigma_y^*}$
No correction	706 ± 160 nm
One-to-one + DFS	137 ± 38,0 nm
One-to-one + DFS + knobs	4.82 ± 0.570 nm

Orbit corrections and knobs reduce the beam size by a factor 147.

Impact of short-range wakefields in the CLIC 380 GeV BDS

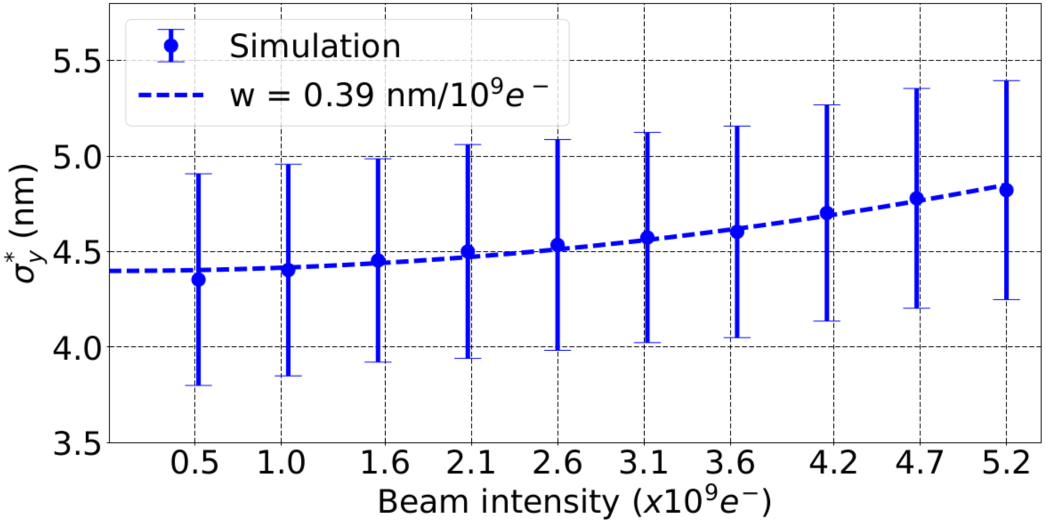

Figure : Vertical IP beam size σ_y^* vs. beam intensity in the 380 GeV BDS, calculated with PLACET with wakefields.

$$w\,[nm/10^9\,e] = \frac{\left(\sqrt{\sigma_{y,q}^2 - \sigma_{y,0}^2}\right)}{q}$$

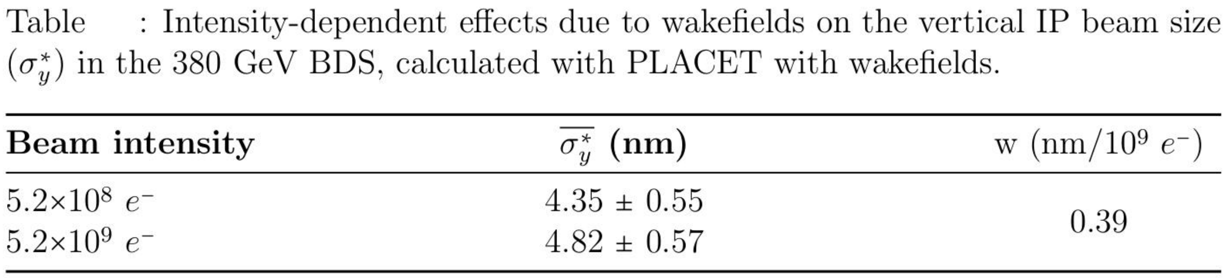

Table : Intensity-dependent effects due to wakefields on the vertical IP beam size (σ_y^*) in the 380 GeV BDS, calculated with PLACET with wakefields.

Beam intensity	$\overline{\sigma_y^*}$ **(nm)**	w (nm/10^9 e^-)
5.2×10^8 e^-	4.35 ± 0.55	0.39
5.2×10^9 e^-	4.82 ± 0.57	

Short-range wakefields have a slight effect in the 380 GeV BDS.

Simulations of the impact of long-range wakefields in CLIC

In the CLIC 380 GeV BDS

Long-range wakefields in the CLIC BDS
Resistive walls wakefield

- Electrons going through the pipe interacts with the surrounding structure and generates a wake field.
- This wake field produces a transverse kick for the following bunches.
- The following model is used for the transverse wake function:

$$W(z)=\frac{c}{\pi b^3}\sqrt{\left(\frac{Z_0}{\sigma_r \pi z}\right)}L$$

With b the radius of the beam pipe, Z_0 the impedance of the vacuum, σ_r the conductivity of the pipe and L the length of the beam line element.

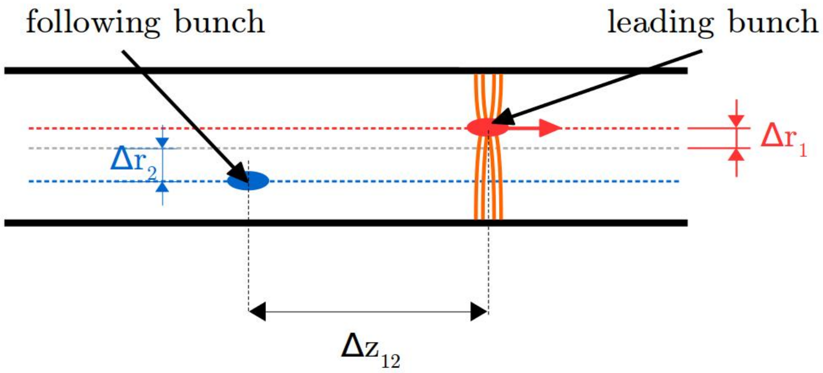

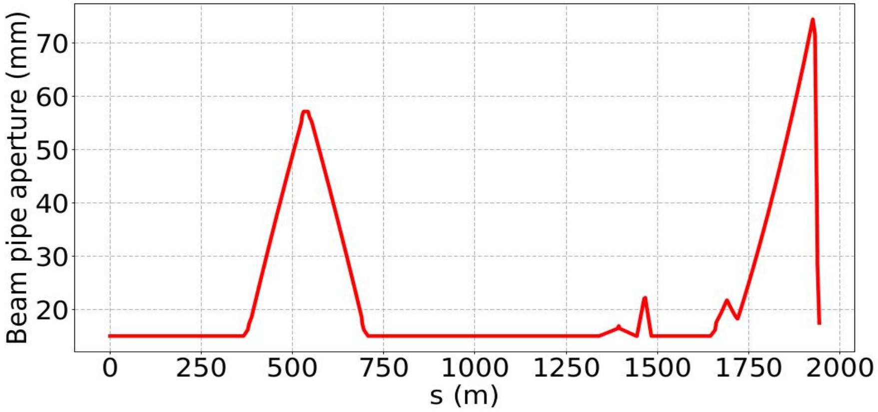

Figure: The CLIC BDS beam aperture profile.

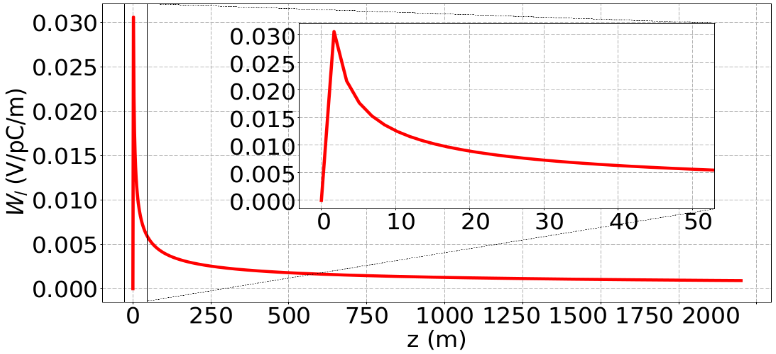

Figure : The CLIC resistive walls wakepotential for a copper beam pipe with a constant radius of 15 mm for the length of the CLIC BDS (~1949 m). The zoom shows the wakepotential for the length of a train (~ 52.8 m).

The long-range wakefield sources taken into account are the resistive walls.

Impact of long-range wakefields in the 380 GeV CLIC BDS

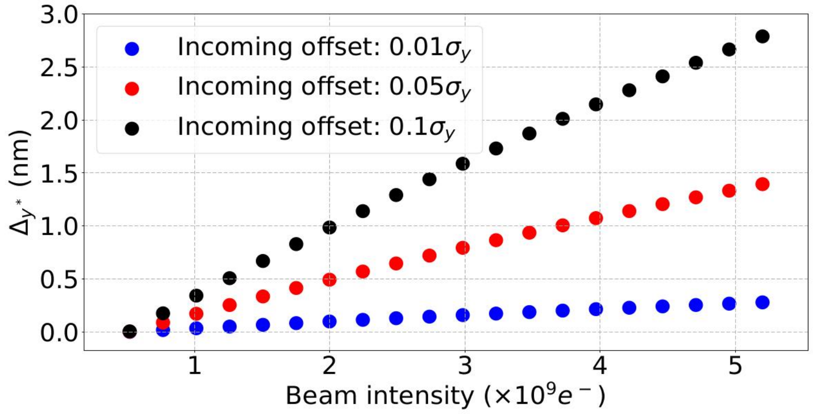

Figure : Vertical orbit deflection at the IP between the first and last bunch of a train Δy^* vs. beam intensity for three incoming constant position offsets of the train of bunches in the 380 GeV CLIC BDS: $0.01\sigma_y$, $0.05\sigma_y$ and $0.1\sigma_y$, calculated with PLACET with resistive walls.

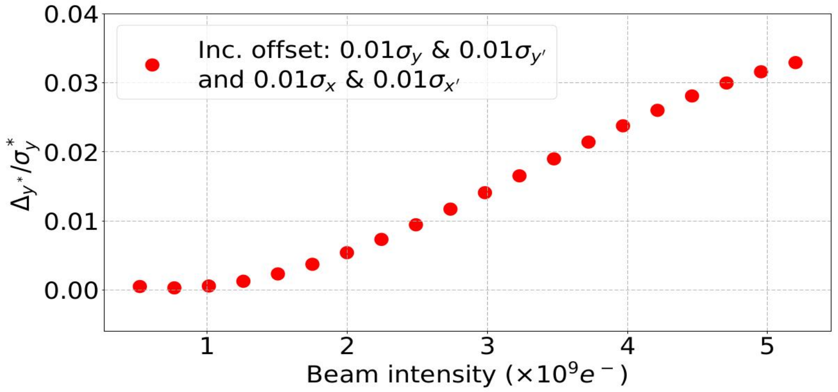

Figure : Vertical orbit deflection at the IP between the first and last bunch of a train normalised by the IP vertical beam size ($\Delta y^*/\sigma_y^*$) vs. beam intensity for a train with incoming constant horizontal position and angle offsets of respectively $0.01\sigma_x$ and $0.01\sigma_{x'}$ and vertical incoming position and angle offsets of respectively $0.01\sigma_y$ and $0.01\sigma_{y'}$ in the 380 GeV CLIC BDS, calculated with PLACET with resistive walls.

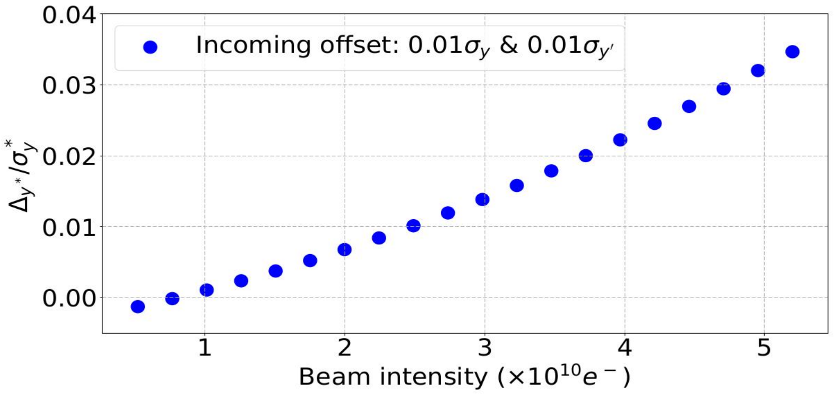

Figure : Vertical orbit deflection at the IP between the first and last bunch of a train normalised by the IP vertical beam size ($\Delta y^*/\sigma_y^*$) vs. beam intensity for a train with incoming constant horizontal position and angle offsets of respectively $0.01\sigma_x$ and $0.01\sigma_{x'}$ and vertical incoming position and angle offsets of respectively $0.01\sigma_y$ and $0.01\sigma_{y'}$ in the 380 GeV GeV BDS, calculated with PLACET with resistive walls.

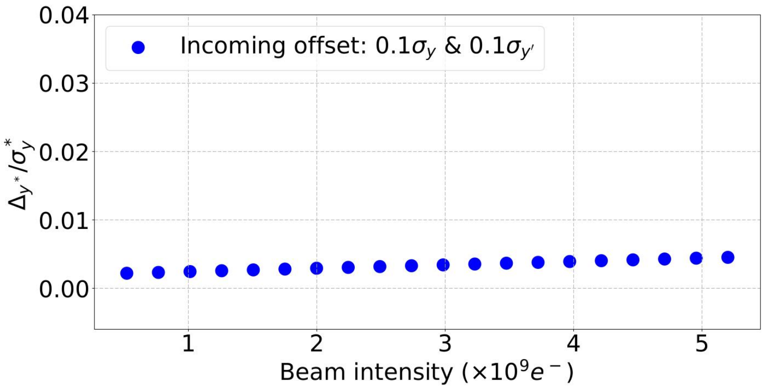

Figure Vertical orbit deflection at the IP between the first and last bunch of a train normalised by the IP vertical beam size ($\Delta y^*/\sigma_y^*$) vs. beam intensity for a train with a random and around zero incoming vertical and horizontal position and angle offsets of between -0.05 and 0.05 σ in the 380 GeV CLIC BDS, calculated with PLACET with resistive walls.

Impact of long-range wakefields in the CLIC 380 GeV BDS
Luminosity

- Study of the impact of luminosity degradation due to the vertical orbit deflection at the IP with Guinea-Pig, a code simulating the impact of beam-beam effects on luminosity and background.

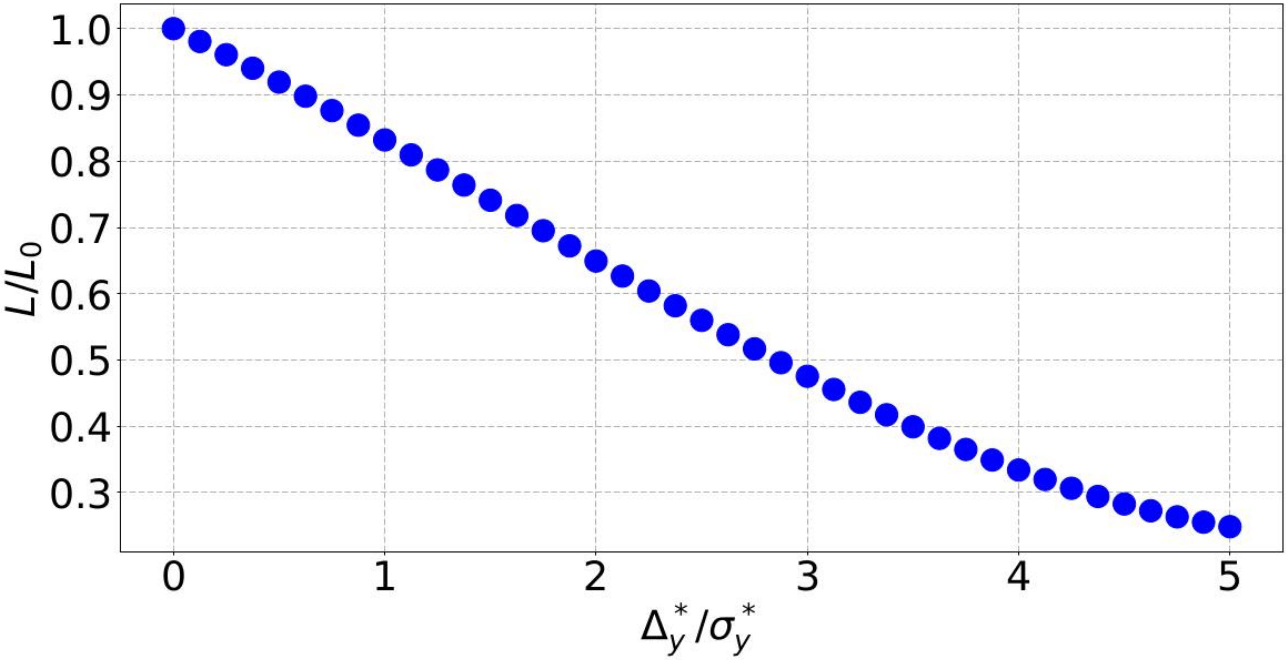

Figure : CLIC 380 GeV BDS luminosity degradation vs. relative vertical offset of the colliding beams.

$$L = f_{coll}\frac{n_1 n_2}{4\pi\sigma_x^*\sigma_y^*}F$$

Impact of long-range wakefields in the CLIC 380 GeV BDS

Summary

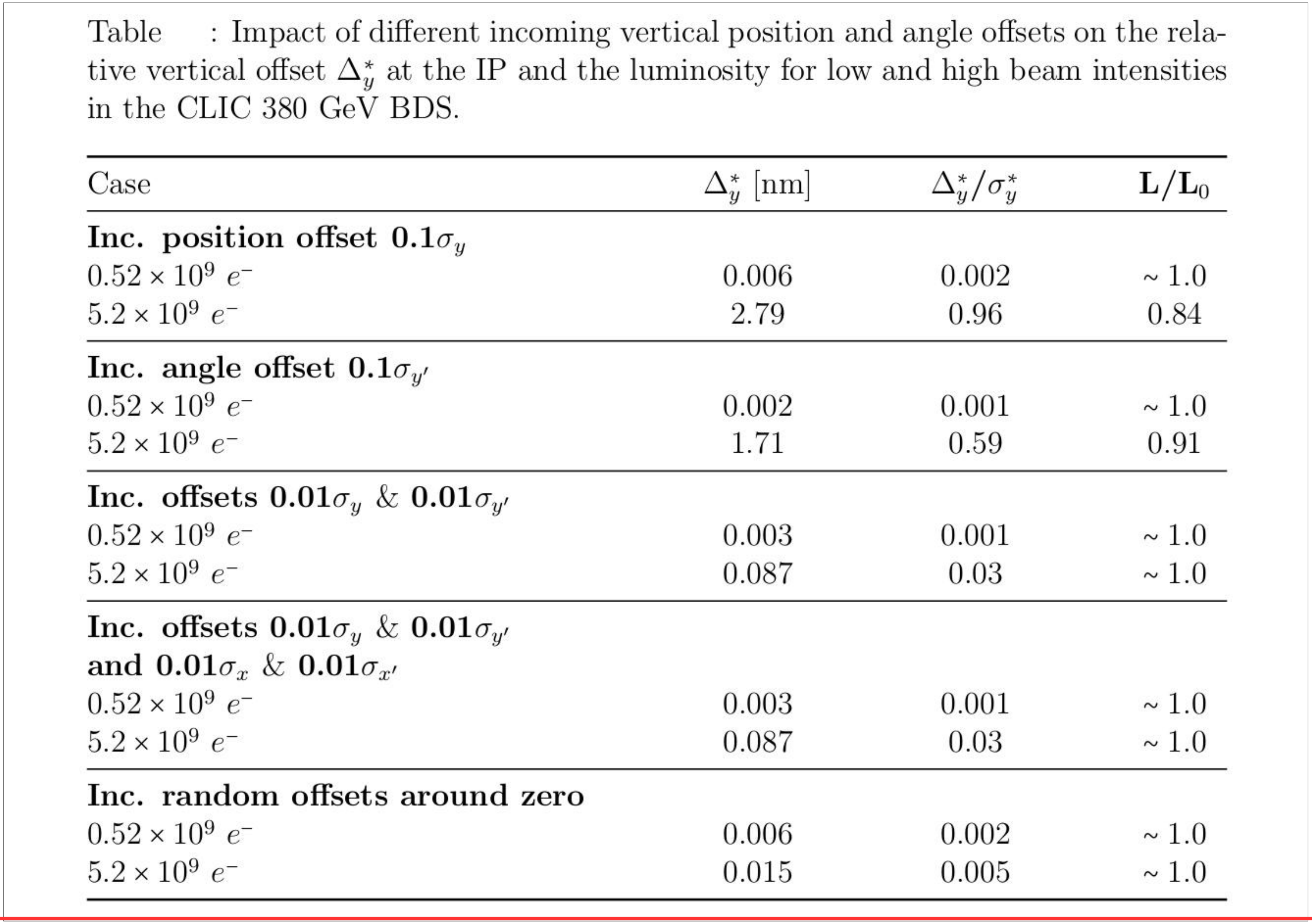

Table : Impact of different incoming vertical position and angle offsets on the relative vertical offset Δ_y^* at the IP and the luminosity for low and high beam intensities in the CLIC 380 GeV BDS.

Case	Δ_y^* [nm]	Δ_y^*/σ_y^*	$\mathbf{L/L_0}$
Inc. position offset 0.1σ_y			
0.52×10^9 e^-	0.006	0.002	~ 1.0
5.2×10^9 e^-	2.79	0.96	0.84
Inc. angle offset 0.1$\sigma_{y'}$			
0.52×10^9 e^-	0.002	0.001	~ 1.0
5.2×10^9 e^-	1.71	0.59	0.91
Inc. offsets 0.01σ_y & 0.01$\sigma_{y'}$			
0.52×10^9 e^-	0.003	0.001	~ 1.0
5.2×10^9 e^-	0.087	0.03	~ 1.0
Inc. offsets 0.01σ_y & 0.01$\sigma_{y'}$ and 0.01σ_x & 0.01$\sigma_{x'}$			
0.52×10^9 e^-	0.003	0.001	~ 1.0
5.2×10^9 e^-	0.087	0.03	~ 1.0
Inc. random offsets around zero			
0.52×10^9 e^-	0.006	0.002	~ 1.0
5.2×10^9 e^-	0.015	0.005	~ 1.0

Long-range wakefields have a significant impact in the CLIC 380 GeV BDS. An intra-train feedback system would be necessary in order to achieve the luminosity goals.

Acknowledgements

Special thanks to:

- Philip Burrows from the University of Oxford.
- Andrea Latina and Daniel Schulte from CERN.
- Angeles Faus-Golfe from IJCLab.

Conclusions

- The intensity-dependent effects in ATF2 were quantified with PLACET taking into account several types of wakefield sources and considering realistic static and dynamic imperfections.
- The simulated and measured intensity-dependent parameters seemed to agree really well taking into account realistic simulation conditions in ATF2.
- The intensity-dependent effects due to short-range wakefields are negligible in both the CLIC and ILC BDS.
- The intensity-dependent effects due to long-range wakefields have a significant impact on the luminosity in both CLIC and ILC BDS.
- An intra-train feedback system is necessary in order to correct those effects and to achieve the required luminosity goals. Such a system has been studied to correct the vertical jitters generated by ground motion [8].
- A prototype feedback system was tested in ATF2 and gave promising results [9]. The next step will be to implement this feedback and study its impact on the luminosity losses due to intensity-dependent effects.
- All the details about the intensity-dependent effect studies can be found in my Dphil thesis.

Thank you